

Ligand exchange upon oxidation of a dinuclear Mn complex— detection of structural changes by FT-IR spectroscopy and ESI-MS†

Gerriet Eilers,^a Camilla Zettersten,^b Leif Nyholm,^{‡,b} Leif Hammarström^a and Reiner Lomoth^{*a}

^a Department of Physical Chemistry, Uppsala University, BOX 579, S-75123, Uppsala, Sweden.
E-mail: Reiner.Lomoth@fki.uu.se

^b Department of Analytical Chemistry, Uppsala University, BOX 599, S-75124, Uppsala, Sweden

Received 30th September 2004, Accepted 31st January 2005

First published as an Advance Article on the web 15th February 2005

The structural rearrangements triggered by oxidation of the dinuclear Mn complex $[\text{Mn}_2(\text{bpmp})(\mu\text{-OAc})_2]^+$ (bpmp = 2,6-bis[bis(2-pyridylmethyl)amino]methyl-4-methylphenol anion) in the presence of water have been studied by combinations of electrochemistry with IR spectroscopy and with electrospray ionization mass spectrometry (ESI-MS). The exchange of acetate bridges for water (D_2O) derived ligands in different oxidation states could be monitored by mid-IR spectroscopy in $\text{CD}_3\text{CN}-\text{D}_2\text{O}$ mixtures following the $\nu_{\text{as}(\text{C}-\text{O})}$ bands of bound acetate at 1594.4 cm^{-1} (II,II), 1592.0 cm^{-1} (II,III) and 1586.5 cm^{-1} (III,III). Substantial loss of bound acetate occurs at much lower water content ($< 0.5\%$ v/v) in the III,III state than in the II,II and II,III states ($\geq 10\%$). The ligand-exchange reactions do not initially reduce the overall charge of the complex but facilitate further oxidation by proton-coupled electron transfer as the water-derived ligands are increasingly deprotonated in higher oxidation states. In the IR spectra deprotonation could be followed by the formation of acetic acid (DOAc, $\sim 1725\text{ cm}^{-1}$, $\nu_{(\text{C}=\text{O})}$) from the released acetate (1573.6 cm^{-1} , $\nu_{\text{as}(\text{C}-\text{O})}$). By the on-line combination of an electrochemical flow cell with ESI-MS several product complexes could be identified. A di- μ -oxo bridged III,IV dimer $[\text{Mn}_2(\text{bpmp})(\mu\text{-O})_2]^{2+}$ (m/z 335.8) can be generated at potentials below the III,III/II,III couple of the di- μ -acetato complex (0.61 V vs. ferrocene). The ligand-exchange reactions allow for three metal-centered oxidation steps to occur from II,II to III,IV in a potential range of only 0.5 V, explaining the formation of a spin-coupled III,IV dimer by photo-oxidation with $[\text{Ru}(\text{bpy})_3]^{3+}$ in previous EPR studies.

Introduction

Synthetic Mn complexes have been extensively studied as structural models for the active site of metalloenzymes like catalase or the oxygen evolving center of photosystem II (PSII).^{1–5} The active site metal center of PSII goes through several oxidation states as it couples single electron transfer steps to multiple electron catalytic reactions. Subsequent oxidations of the synthetic complexes, however, are typically separated by several hundreds of mV. This imposes severe problems for applications as functional mimics in artificial photosynthesis,^{6–11} since photo-oxidation of the Mn complex, even with strong oxidants as $[\text{Ru}(\text{bpy})_3]^{3+}$ ($E^0 \sim 1.3\text{ V vs. SCE}$), is difficult to achieve more than once or twice before further oxidation becomes thermodynamically infeasible or results in oxidative degradation of the ligand. In the natural reaction center of PSII^{12,13} all four oxidation steps of the Mn cluster needed for water oxidation are compressed in about 0.3 V only. This narrow potential range is a result of deprotonation reactions that provide charge compensation in response to the oxidation steps. Therefore, reactions that compensate for the increasing charge on the metal centers are most probably indispensable for a functional mimic.

For some synthetic Mn complexes proton-coupled electron transfer has been reported and the potentials for oxidation of the oxo-bridged Mn dimers have been shown to drop by several hundreds of mV in response to deprotonation.^{14,15} The transformation of a terminal aquo ligand into an oxo bridge

upon oxidation of a $\text{Mn}_2(\text{II,II})$ complex has also been reported representing a more special case of charge compensation by deprotonation.¹⁶ Charge compensating exchange of ligands is also observed in the catalytic disproportionation of H_2O_2 by di(μ -carboxylato) $\text{Mn}_2(\text{II,II})$ complexes where the exchange of acetate bridges for oxo ligands leads to the active di(μ -oxo) $\text{Mn}_2(\text{III,IV})$ species.¹⁷

For the dimeric $\text{Mn}_2(\text{II,II})$ complex $[\text{Mn}_2(\text{bpmp})(\mu\text{-OAc})_2]^+$ (**1a**) {bpmp[−] is the anion of 2,6-bis[bis(2-pyridylmethyl)amino]methyl-4-methylphenol} oxidation to a $\text{Mn}_2(\text{III,IV})$ complex has been accomplished by photo generated $[\text{Ru}(\text{bpy})_3]^{3+}$.^{18,19} Stepwise oxidation of $[\text{Mn}_2(\text{bpmp})(\mu\text{-OAc})_2]^+$ by electron transfer to the oxidized sensitizer could account for the formation of $[\text{Mn}_2(\text{bpmp})(\mu\text{-OAc})_2]^{2+}$ (**1b**) and $[\text{Mn}_2(\text{bpmp})(\mu\text{-OAc})_2]^{3+}$ (**1c**) with the potentials of the II,III/II,II and III,III/II,III couples well below the oxidant. Further oxidation of the same complex beyond the III,III state is however impossible and the third oxidation step resulting in a III,IV complex must rely on precedent rearrangements of the ligand set. Since the formation of the $\text{Mn}_2(\text{III,IV})$ dimer was observed only in partly aqueous solutions it was proposed that in higher oxidation states the exchange of acetate bridges (OAc^-) for more negative oxo (O^{2-}) ligands might provide the charge compensation needed for a third oxidation step to occur below the oxidation potential of the $[\text{Ru}(\text{bpy})_3]^{3+}$ oxidant.^{18,19} A mono- or di- μ -oxo bridging motif was suggested but the structure of the $\text{Mn}_2(\text{III,IV})$ dimer and the mechanism of its formation could not be revealed from the EPR data.

In this paper we describe an investigation of the structural rearrangements of $[\text{Mn}_2(\text{bpmp})(\mu\text{-OAc})_2]^{n+}$ ($n = 1, 2, 3$) in the presence of water by combinations of electrochemistry with IR spectroscopy and with electrospray ionization mass spectrometry (ESI-MS). By mid-IR spectroelectrochemistry we were able to monitor the loss of acetate ligands in the II,II; II,III and III,III state as well as the release of protons from bound water in response to oxidation. Further information on the product structures was obtained by the on-line combination

† Electronic supplementary information (ESI) available: Fig. S1: Spectroelectrochemical changes upon oxidation of $[\text{Mn}^{\text{II,II}}_2(\text{bpmp})(\mu\text{-OAc})_2]^+$ in CD_3CN . Fig. S2: IR spectra of $[\text{Mn}^{\text{II,II}}_2(\text{bpmp})(\mu\text{-OAc})_2][\text{ClO}_4]$ and $[\text{Mn}^{\text{II,II}}_2(\text{bpmp})(\mu\text{-OAc})_2][\text{ClO}_4]_2$ in the solid state and in CD_3CN . Fig. S3: Selected full range EC-ESI-MS spectra of $[\text{Mn}^{\text{II,II}}_2(\text{bpmp})(\mu\text{-OAc})_2]^+$. See <http://www.rsc.org/suppdata/dt/b4/b415148h/>

‡ Current address: Department of Materials Chemistry, Uppsala University, BOX 538, S-75121, Uppsala, Sweden.

of an electrochemical flow cell with ESI-MS.^{20–22} This method was now employed for the first time for the *in situ* detection of ligand-exchange products formed upon oxidation of a metal complex. By this approach a number of ligand-exchanged dimers formed in response to oxidation of $[\text{Mn}_2(\text{bpmp})(\mu\text{-OAc})_2]^+$ could be identified including a III,IV dimer with a m/z value consistent with the complex $[\text{Mn}_2(\text{bpmp})(\mu\text{-O})_2]^{2+}$.

Experimental

Materials

$[\text{Mn}_2(\text{bpmp})(\mu\text{-OAc})_2][\text{ClO}_4]$ and $[\text{Mn}_2(\text{bpmp})(\mu\text{-OAc})_2][\text{ClO}_4]_2$ were provided by Magnus Anderlund and Prof Licheng Sun (Stockholm University, Sweden) and had been prepared according to reported methods.²³

Electrochemistry

Cyclic voltammetry, differential pulse voltammetry and controlled potential electrolysis were carried out using an Autolab potentiostat with an GPES electrochemical interface (Eco Chemie). The working electrode was a glassy carbon disc (diameter 3 mm, freshly polished) for voltammetry or a platinum grid for bulk electrolysis, respectively. A platinum spiral in a compartment separated from the bulk solution by a fritted disk was used as counter electrode. The reference electrode was a non-aqueous Ag^+/Ag electrode (CH Instruments, 0.010 M AgNO_3 in acetonitrile) with a potential of -0.08 V vs. the ferrocenium–ferrocene (Fc^+/Fc) couple in acetonitrile as an external standard. All potentials reported here are vs. the Fc^+/Fc couple by adding -0.08 V to the potentials measured vs. the Ag^+/Ag electrode.

All solutions were prepared from dry acetonitrile (Merck, spectroscopy grade, dried with $\text{MS } 3 \text{ \AA}$) with 0.1 M tetrabutylammonium perchlorate (Fluka, electrochemical grade) as supporting electrolyte that has been dried in vacuum at 383 K. Before all measurements oxygen was removed by bubbling the stirred solutions with solvent-saturated argon and the samples were kept under argon atmosphere during measurements.

IR Spectroscopy

IR absorption spectra were recorded between 1000 and 5000 cm^{-1} at a resolution of 1 cm^{-1} on a Bruker FT-IR spectrometer (IFS 66 v/S) with the sample as a KBr pellet or as solution in a liquid-sample-cell (Bruker A140) between CaF_2 windows and a pathlength of 125 μm .

The solutions were prepared in CD_3CN (Aldrich, 99.8 atom% D) or mixtures of CD_3CN with D_2O (Aldrich, 99.9 atom% D). With the deuterated solvents and KPF_6 (0.1 M) as supporting electrolyte the background absorption in the range of the carboxylate bands (1800–1200 cm^{-1}) was minimized and could be subtracted for D_2O contents of $\leq 75\%$ (v/v). Minor differences in residual H_2O content between sample and background measurement gave rise to incomplete background correction in some spectra. Where necessary the remaining absorption bands of H_2O (1632 cm^{-1} , $\delta_{(\text{H}-\text{O}-\text{H})}$) and HOD (1432 cm^{-1} , $\delta_{(\text{H}-\text{O}-\text{D})}$) were subtracted from the presented spectra.

Higher oxidation states of the complex were prepared by exhaustive electrolysis of $[\text{Mn}_2(\text{bpmp})(\mu\text{-OAc})_2][\text{ClO}_4]$ (6 mM) in CD_3CN . After electrolysis the samples were diluted 1 : 1 with CD_3CN or $\text{CD}_3\text{CN}-\text{D}_2\text{O}$ mixtures to allow for the variation of the D_2O -concentration while keeping the concentration of the complex constant.

IR spectroelectrochemical measurements were performed on solutions of $[\text{Mn}_2(\text{bpmp})(\mu\text{-OAc})_2][\text{ClO}_4]$ (6 mM) in CD_3CN or $\text{CD}_3\text{CN}-\text{D}_2\text{O}$ with KPF_6 (0.1 M). The spectra were recorded in absorption mode in a thin layer cell equipped with CaF_2 windows and the optical path length set to 125 μm . The working

electrode was a Pt grid (1024 meshes cm^{-2} , 65% open area). The counter electrode was a Pt cylinder concentric with the working electrode and sufficiently separated from the thin layer compartment to ensure that no electrolysis product from the counter electrode can diffuse into the analysed volume on the timescale of the experiments. The reference electrode was of the same type as described for electrochemistry and connected to the cell *via* a salt bridge (0.5 M KPF_6 in CD_3CN).

CD_3CN , D_2O and KPF_6 were purchased from Sigma–Aldrich. CD_3CN was dried over molecular sieve (3 \AA) prior to use and KPF_6 was dried overnight at 353 K in vacuum.

EC-ESI-MS

A thin layer electrochemical flow cell (Bioanalytical Systems Inc., West Lafayette, IN) was coupled to a PE-Sciex API III+ triple quadrupole mass spectrometer (Concord, ON, Canada) with an IonSpray interface. An isolation transformer (type PVM 440 0019, Tufvassons, Sigtuna, Sweden) was used to decouple the electrochemical cell from the ESI high voltage so the EC cell and the potentiostat (Polarographic Analyzer/Stripping Voltammeter, Model 264, EG&G Princeton Applied Research, Princeton, NJ) were floating on the high voltage. Details of the coupling of the electrochemical thin layer flow cell to the mass spectrometer are described elsewhere.²² Sample solution was introduced to the floating system (isolated from ground by pieces of Styrofoam) by a syringe pump (Syringe Infusion Pump 22, Harvard Apparatus, Inc., Cambridge, MA).

In the electrochemical equipment, the working electrode was a series dual glassy carbon (GC) disc electrode (3 mm diameter) embedded in a PEEK block (Bioanalytical Systems Inc.). The spacer gasket (Bioanalytical Systems Inc.) that was used was 16 μm thin. The stainless steel block of the flow cell was used as a pseudo-reference electrode and a laboratory made stainless steel electrode, which was made to fit the reference electrode compartment of the flow cell, was used as the counter electrode. This modified set-up of the flow cell was made to minimize interferences as a result of the electrochemical reactions occurring at the counter electrode.

Experiments were made in positive electrospray mode. The fused silica spray capillary from the flow cell (250 mm long, 50 μm inner diameter and 184 μm outer diameter, total volume of 0.49 μL , Polymicro Technologies, Phoenix, AZ) to the mass spectrometer was centered in a stainless steel capillary counter assembly delivering 0.7 L min^{-1} of air (zero grade, generated in house) for pneumatically assisted ESI-MS. The flow rate of dry nitrogen counter-current curtain gas (99.999% purity, 5.0, AGA, Stockholm, Sweden), which was heated to 63 $^\circ\text{C}$, was 1.2 L min^{-1} over the sampling orifice. Mass spectrometric parameters: ion spray voltage (ISV) 3400 V, interface plate voltage (IN) 650 V, orifice lens voltage (OR) 35 V, and AC entrance rod (R0) 30 V. About 30 scans between m/z 150–900 or 1000 (step size 0.2), with a dwell time of 1.0 ms and pause time of 0.052 ms, were recorded in multichannel acquisition (MCA) mode during 1.97 min. Data were collected on a Macintosh computer by the Tune2.5-FPU software and analyzed by Multiview 68 K 1.3.

The use of supporting electrolyte was limited by the suppression effect^{24–27} from the TBA^+ ions on the analyte ions in the electrospray process. This required relatively high concentrations of the analyte to replace most or the entire supporting electrolyte in the EC-MS experiments. The measurements were performed with 45 μM $[\text{Mn}_2^{\text{III}}(\text{bpmp})(\mu\text{-OAc})_2][\text{ClO}_4]$ in acetonitrile and 97 μM $[\text{Mn}_2^{\text{III}}(\text{bpmp})(\mu\text{-OAc})_2][\text{ClO}_4]$, 25 μM TBAP in acetonitrile–water solution. Under these conditions conductivity was sufficient for the EC cell while suppression effects were avoided.

Samples were pumped through the thin layer electrochemical flow cell at a flow rate of 10 $\mu\text{L min}^{-1}$ in acetonitrile–water and 5 $\mu\text{L min}^{-1}$ in the less conductive acetonitrile solution where the flow rate was reduced to obtain a stable electrospray.

Results and discussion

Cyclic voltammetry

In dry acetonitrile, cyclic voltammograms of $[\text{Mn}_2(\text{bpmp})(\mu\text{-OAc})_2]^+$ show two quasi-reversible waves that have been attributed earlier to the $\text{Mn}_2(\text{II,III})/\text{Mn}_2(\text{II,II})$ ($E_{1/2}(1) = 0.06$ V vs. $\text{Fc}^{+/0}$) and $\text{Mn}_2(\text{III,III})/\text{Mn}_2(\text{II,III})$ ($E_{1/2}(2) = 0.61$ V) couples, respectively^{18,23,28} (see Fig. 1(b)). The potential and chemical reversibility of the first process is nearly unaffected by the presence of water ($v/v \leq 10\%$)¹⁸ (Fig. 1(a)). The peak current is only somewhat diminished and the peak split slightly increased in acetonitrile/water (90 : 10) as compared to neat acetonitrile. The second oxidation wave, however, becomes broader and chemically irreversible when changing from acetonitrile to acetonitrile–water mixtures. On the reverse CV scans extending to sufficiently negative potential an additional cathodic peak is observed at -0.25 V provided that water is present and that the second oxidation step was accomplished in the forward scan (Fig. 1(a), bold line). This peak occurs at a potential more negative than the re-reduction of $[\text{Mn}_2^{\text{II,III}}(\text{bpmp})(\mu\text{-OAc})_2]^{2+}$ to $[\text{Mn}_2^{\text{II,II}}(\text{bpmp})(\mu\text{-OAc})_2]^+$ but in subsequent scans no counter peak is observed on the forward scans and peak heights of the original oxidation peaks are unaffected by repeated scanning.

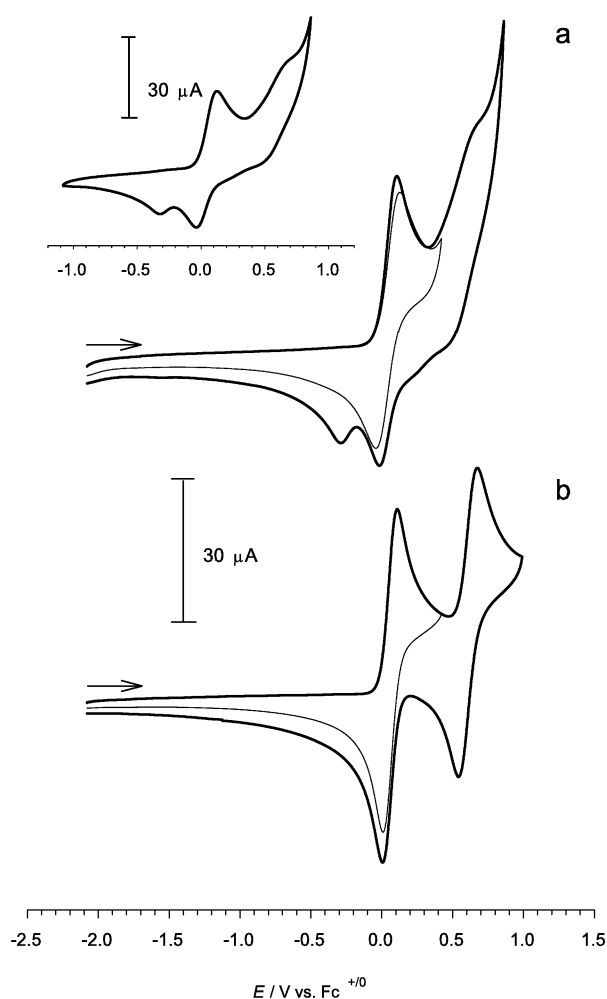


Fig. 1 Cyclic voltammograms (0.100 V s^{-1}) of **1a** (2 mM) in CH_3CN with 10% (v/v) of water (a) and neat CH_3CN (b) with 0.1 M $[(n\text{-C}_4\text{H}_9)\text{N}][\text{ClO}_4]$ as supporting electrolyte. Inset: Second scan.

The effects of water on the electrochemical behavior of $[\text{Mn}_2(\text{bpmp})(\mu\text{-OAc})_2]^+$ can be rationalized in terms of ligand-exchange reactions. The rather small effect on the first voltammetric wave demonstrates that with a water content up to 10% only a minor fraction of the initial II,II state undergoes ligand-exchange reactions. The reversibility of the first oxidation and

the absence of additional voltammetric peaks on the second oxidation scan indicates that also the II,III state has little reactivity towards water.

The irreversibility of the second wave and the new peak on the reverse scan clearly demonstrate the effect of water on the III,III state. Assigning the irreversibility tentatively to a charge compensating ligand-exchange reaction (see below) the new cathodic peak can be attributed to the reduction of one of the products. The new cathodic peak does not have any counterpeak in the second oxidation scan, which indicates that the ligand-exchange product rapidly and quantitatively re-establishes the acetate bridges upon reduction. Another indication for this behavior is that the first oxidation wave reaches the same amplitude in the second scan as in the first scan.

It could be anticipated that ligand-exchange reactions involve the relatively weakly bound acetate bridges. The C–O stretching frequencies of carboxylate ions are known to change upon coordination to a metal center. This provides a probe for the degree of acetate loss from the complex in different oxidation states.

IR Spectroscopy

Band assignments and different redox states in anhydrous acetonitrile. Fig. 2 shows the spectra of the complex in the II,II (a), the II,III (b) and III,III states (c) in anhydrous acetonitrile (CD_3CN) solution together with spectra of the Hbpmp ligand (d), free acetate (as sodium acetate, e) and acetic acid (f). All spectral changes observed upon oxidation of the complex could be fully reversed upon re-reduction in carefully dried acetonitrile and several isosbestic points were preserved in the interconversions (see ESI†). The spectra in Fig. 2 show absolute spectra for the different redox-states rather than difference spectra, because maxima of absorption changes do not represent the maxima in the absolute spectra in the case of overlapping absorption bands.

In the II,II state (Fig. 2(a)) the most intense bands observed at 1594 and 1423 cm^{-1} can be assigned to the asymmetric (ν_{as}) and symmetric stretching (ν_{s}) modes of the acetate ligands though they are superimposed to absorptions of the bpmp[−] ligand (compare with Fig. 2(d)) that arise mainly from ring stretching modes (1571 , 1595 cm^{-1}) of the pyridyl and phenolic groups. The shoulder at 1601 cm^{-1} in the complex corresponds to the band at 1595 cm^{-1} of the Hbpmp ligand that shifts by 6 cm^{-1} upon coordination while the peak at 1594 cm^{-1} can be attributed to the ν_{as} mode of the acetate ligands. This assignment is supported by the spectrum of the complex without acetate ligands (see below).

Oxidation to the II,III state (Fig. 2(b)) shifts both acetate bands to lower frequencies (see Table 1) and decreases the peak intensity of the ν_{as} band. Upon further oxidation to the III,III state both bands shift to even lower frequencies and the intensity of the ν_{as} band is further reduced. The decreasing intensity of the

Table 1 IR band assignments

Compound ^b	$\tilde{\nu}^a/\text{cm}^{-1}$ ($\epsilon/\text{M}^{-1}\text{cm}^{-1}$)		
	Acetate $\nu_{\text{as}}(\text{C-O})$	Acetate $\nu_{\text{s}}(\text{C-O})$	Pyridine, phenol $\nu(\text{C-C})^c$
1a	1594.4 (1870)	1422.0 (670)	1601 ^d (350)
1b	1592.0 (840)	1390.0 (370)	1605 ^d (1000)
1c	1586.5 (700)	1384.4 (270)	1609 ^d (470)
$\text{CH}_3\text{COO}^-^e$	1573.6 (840)	1410.0 (470)	—
CH_3COOD^f	—	1723.5 (730)	—
Hbpmp	—	—	1595.6 (560)

^a ± 0.3 cm^{-1} . ^b In CD_3CN solution. ^c Several ring stretching modes of the aromatic moieties occur in this range: pyridine (1581 , 1598 cm^{-1}), phenol (1598 , 1606 cm^{-1}). ^d Shoulder. ^e $\tilde{\nu}$ and ϵ from fit with lorentzian bands. ^f As sodium acetate. ^g With 10% D_2O .

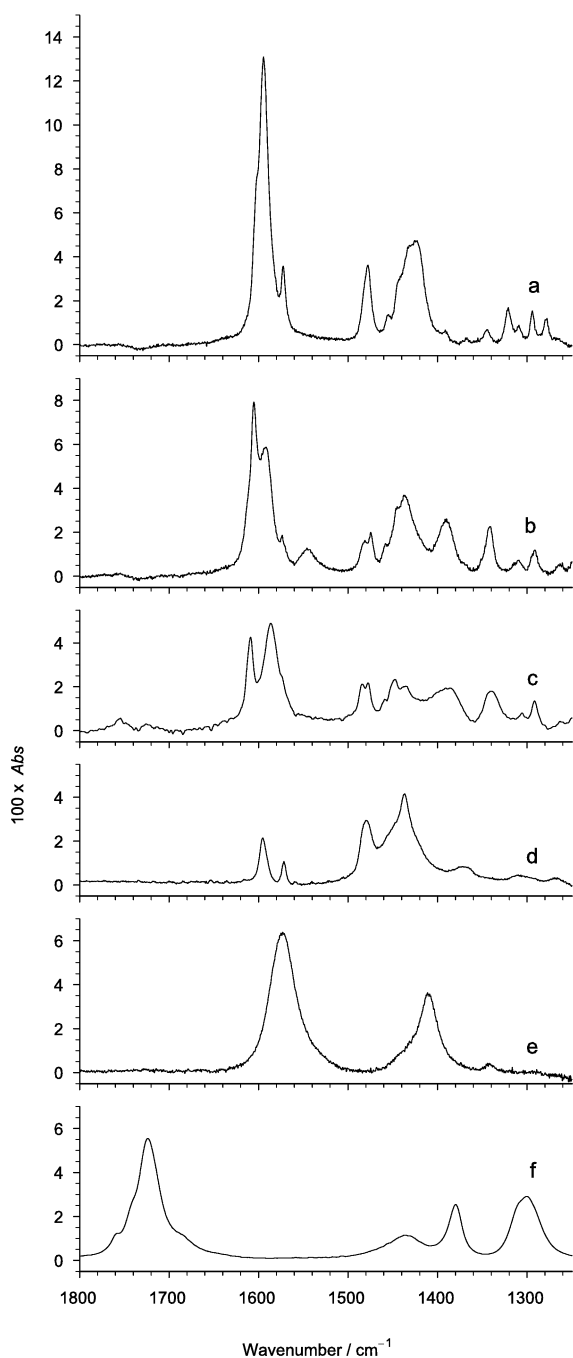


Fig. 2 IR spectra of **1a** (a), **1b** (b) and **1c** (c) obtained by spectroelectrochemistry of $[\text{Mn}_2(\text{bpmp})(\mu\text{-OAc})_2][\text{ClO}_4]$ (3 mM) in CD_3CN with 0.5 M KPF_6 . IR spectra of Hbpmp (3 mM in CD_3CN) (d), NaOAc (6 mM in CD_3CN) (e) and DOAc (6 mM HOAc in CD_3CN with 10% (v/v) D_2O) (f).

ν_{as} band in the higher oxidation states can not be attributed to loss of bound acetate as the ν_{s} band is about equally intense in all oxidation states and no major spectral contributions of free acetate or acetic acid (compare with Fig. 2(e)) are observed.

The separation $\Delta\tilde{\nu} = \tilde{\nu}_{\text{as}} - \tilde{\nu}_{\text{s}}$ is usually correlated to the coordination mode of carboxylate ligands²⁹ and the value of 171 cm^{-1} of the II,II state would be in agreement with bridging coordination. In the II,III and III,III states $\Delta\tilde{\nu}$ increases to 203 and 201 cm^{-1} , respectively, and values of $\Delta\tilde{\nu} \geq 200\text{ cm}^{-1}$ are generally considered to indicate monodentate coordination. However, it has been shown that $\Delta\tilde{\nu}$ for bridging acetate can largely depend on metal oxidation state of isostructural Mn complexes^{30–32} and the simple $\Delta\tilde{\nu}$ criterion has been questioned.³³ In the solid state bridging coordination is evident from X-ray crystallography of the II,II ³⁴ and II,III ²³ state and IR spectra of the solid materials

(ESI[†]) are identical to the spectra in solution with $\Delta\tilde{\nu} \geq 200\text{ cm}^{-1}$ also for the solid II,III material. Thus, the spectra in Fig. 2(a)–(c) are all assigned to bis- μ -acetato bridged complexes and the different frequencies, intensities, and values of $\Delta\tilde{\nu}$ are attributed to the direct effect of metal oxidation state rather than changes in coordination mode. In all three oxidation states the frequencies of these bands (see Table 1), in particular of the ν_{as} band, are distinctly different from those of the free acetate ion (and acetic acid, Fig. 2(f)), allowing quantitative monitoring of the loss of acetate ligands in the presence of water.

Effect of water on the II,II state. Fig. 3 shows the spectrum of $[\text{Mn}_2(\text{bpmp})(\mu\text{-OAc})_2]^+$ in dry acetonitrile and spectra obtained in mixtures with 10, 30, 50, 70 and 90% D_2O . The 90% D_2O spectrum does not extend below 1500 cm^{-1} because of excessive solvent absorption impeding proper background correction. The peaks at 1594 and 1423 cm^{-1} assigned to the ν_{as} and ν_{s} modes of acetate bound to the II,II complex decrease with increasing water content, while the absorption of free acetate increases concomitantly as indicated by the arrows. The ν_{as} band of free acetate accounts for the peak around 1560 cm^{-1} while the ν_{s} band gives rise to the increase in absorption around 1400 cm^{-1} . With 90% water the ν_{as} band of bound acetate disappears almost completely and the intensity of the band at 1560 cm^{-1} corresponds to almost two equivalents of free acetate. From this data it can be concluded that basically all acetate bound to the II,II complex is released as free ions at a water content of 90%. The remaining peak at 1607 cm^{-1} in the spectra with 70 and 90%

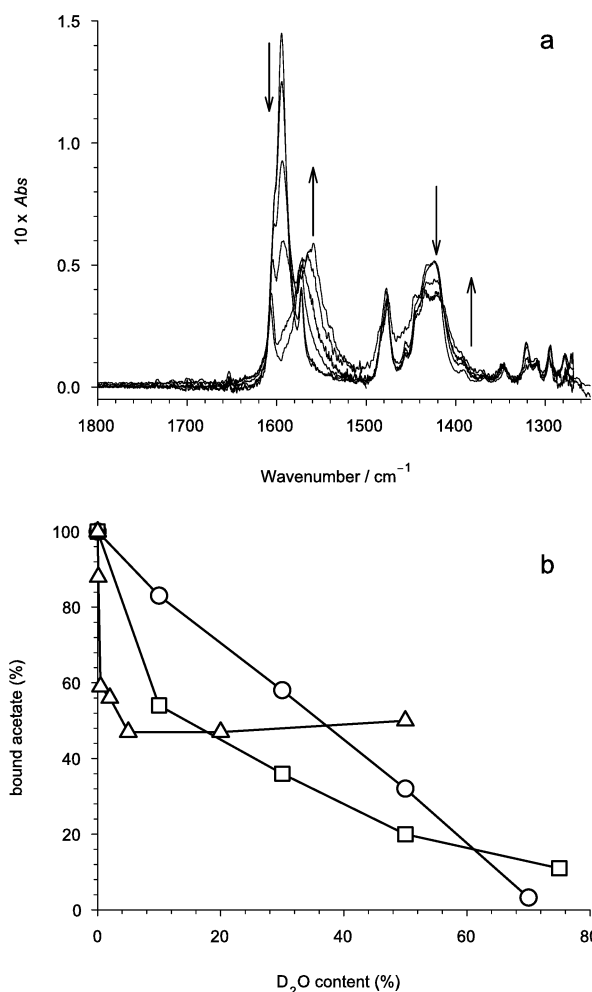


Fig. 3 (a) IR spectra of $[\text{Mn}_2^{\text{II,II}}(\text{bpmp})(\mu\text{-OAc})_2]^+$ (3 mM) in CD_3CN and in $\text{CD}_3\text{CN}\text{-D}_2\text{O}$ mixtures with 10, 30, 50, 70 and 90% (v/v) D_2O (0.1 v/v% D_2O is equivalent to 55 mM D_2O). Arrows indicate increasing D_2O content. (b) Absorbance of bound acetate (ν_{as}) with increasing water content in the II,II (○), II,III (□) and III,III (Δ) state.

D₂O corresponds to the shoulder on the ν_{as} bands in anhydrous solution. It can be attributed to a vibration of the bpmp ligand that occurs at 1595 cm⁻¹ in Hbpmp and is shifted to 1607 cm⁻¹ upon coordination to the manganese. Based on this assignment the IR spectra provide evidence that even so the acetate bridges are lost the Mn ions are still bound to the bpmp ligand.

In agreement with the electrochemistry results most of the complex is found intact at 10% water with less than 15% of the bound acetate being lost. If the partial loss of absorption from bound acetate at lower water contents is arising from the loss of one or both acetate ligands per complex can not be elucidated from the IR data. Fig. 3(b) shows a plot of the absorption from bound acetate *vs.* water concentration. The sharp ν_{as} band of bound acetate is the most reliable indicator for the loss of acetate as the broader band of free acetate is more overlapping with other absorptions and the shape of the acetic acid band depends on the solvent composition (see Figs. 4(a) and 5(a)). For the II,II state the decrease of bound acetate *vs.* water concentration is nearly linear (Fig. 3(b)). Such a behavior can not be rationalized in terms of a simple ligand-exchange equilibrium. This is not surprising, since the equilibrium constant itself would change with such a large change in solvent composition. From the IR data we can not decide whether water coordinates to manganese as acetate ligands are lost. Since no acetic acid is observed, as in higher oxidation states (see below), water would have to bind to the II,II complex as aquo rather than hydroxo or oxo ligand.

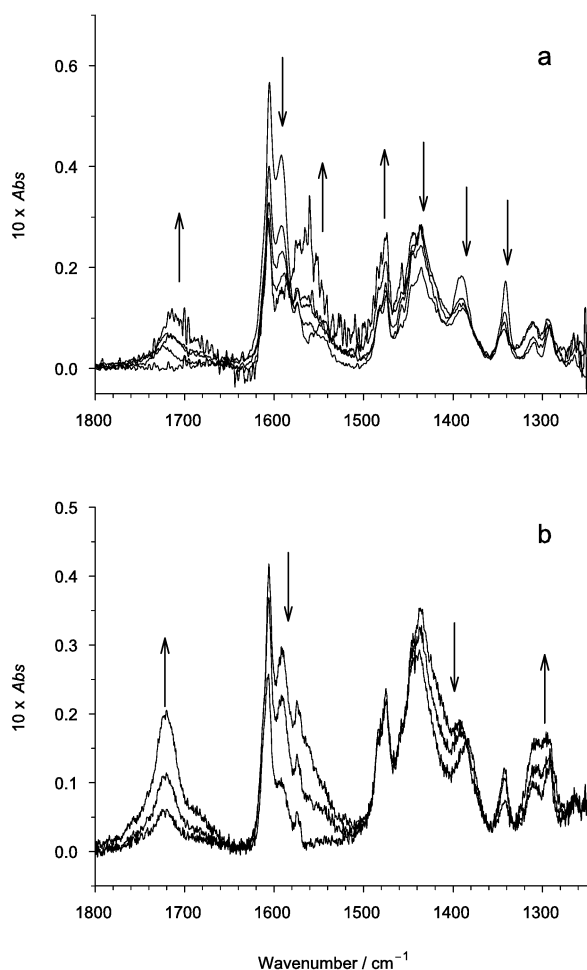


Fig. 4 (a) IR spectrum of [Mn₂^{III,III}(bpmp)(μ-OAc)₂]²⁺ (3 mM) generated by bulk electrolysis (0.32 V) in CD₃CN and spectra with 10, 30, 50 and 75% (v/v) D₂O added *after* electrolysis. Arrows indicate increasing D₂O content. (b) Spectroelectrochemical changes during oxidation (0.32 V) of [Mn₂^{II,III}(bpmp)(μ-OAc)₂]⁺ (3 mM) in CD₃CN with 10% (v/v) D₂O. Arrows indicate increasing time of electrolysis (35, 80, 1200 s).

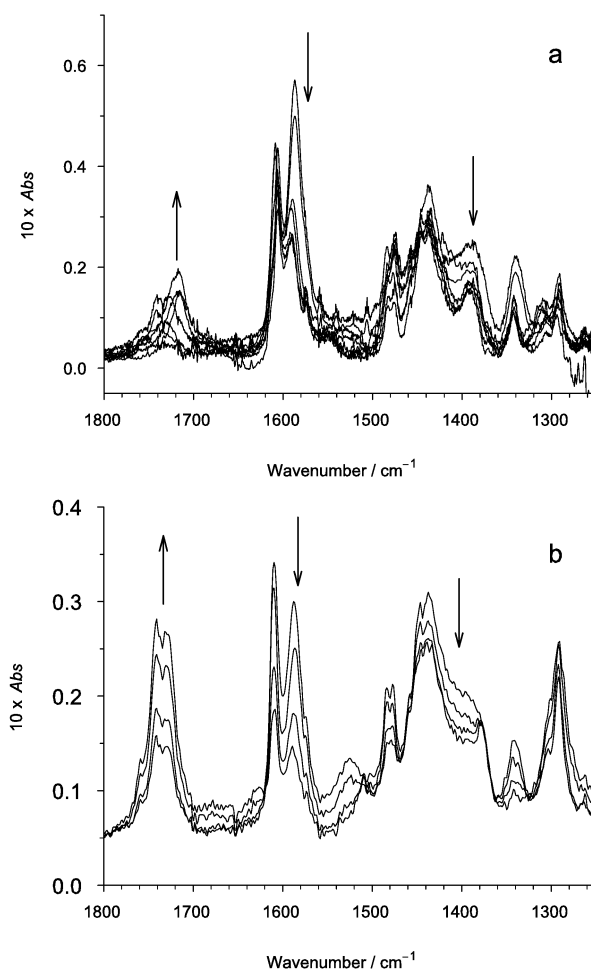


Fig. 5 (a) IR spectrum of [Mn₂^{III,III}(bpmp)(μ-OAc)₂]²⁺ (3 mM) generated by bulk electrolysis (0.82 V) in CD₃CN and spectra with 0.1, 0.5, 2, 5, 20 and 50% (v/v) D₂O added *after* electrolysis. Arrows indicate increasing D₂O content. (b) Spectroelectrochemical changes during oxidation (0.82 V) of [Mn₂^{II,III}(bpmp)(μ-OAc)₂]⁺ (3 mM) in CD₃CN with 1% (v/v) D₂O. Arrows indicate increasing time of electrolysis (20, 100, 600, 1080 s).

For the higher oxidation states the effect of water was studied in two different ways: in one approach water was added *after* exhaustive bulk electrolysis to the II,III or III,III state in dry acetonitrile or, alternatively, to the chemically oxidized preparation of the II,III complex. In the other approach water was added to the solution of the II,II complex *prior* to electrolysis in the spectroelectrochemical cell. With the first approach a simpler situation is created where potential ligand-exchange reactions are restricted to the oxidation state prepared by the initial electrolysis. The latter approach, however, includes the possibility of further oxidation of ligand-exchange products if the potential for this process comes close to or drops below the electrode potential that is continuously applied.

Note that after complete electrolysis no spectral changes were observed for at least 20 min, in any of the redox states, with any of the solvent compositions.

Effect of water on the II,III state. Fig. 4(a) shows the spectrum of [Mn₂(bpmp)(μ-OAc)₂]²⁺ in dry acetonitrile and spectra obtained in mixtures with 10, 30, 50 and 75% D₂O added *after* oxidation. The increasing loss of acetate ligands with increasing water concentration (see also Fig. 3(b)) is evidenced by the depletion of the 1592 cm⁻¹ band that arises from the ν_{as} mode of the bound acetate. Concomitantly rising absorptions around 1560 and 1720 cm⁻¹ are observed indicating that part of the released acetate is protonated. At the highest water content basically all bound acetate is released and the absorption of free acetate amounts to about two thirds of two equivalents of acetate

while the acetic acid approximately accounts for the remaining third. Exact quantification of acetic acid is difficult however due to the variation of the spectrum with D₂O content. These results show that the exchange of acetate for water in the II,III complex is accompanied by deprotonation of the binding water as a charge compensation for the higher metal oxidation state. Assuming that all protons released in this process result in the formation of acetic acid we can estimate that *on average* not more than one proton is released per complex.

In a complementary experiment (see Fig. 4(b)) 10% D₂O was added to a solution of the II,II complex *before* electrolysis at 0.32 V that oxidized the intact complex to the II,III state. With this water content only about 15% of the II,II complex undergoes ligand exchange (see above). Thus, electrolysis under these conditions oxidizes predominantly the intact complex.

In the spectroelectrochemical thin-layer cell, exhaustive electrolysis occurs in less than 30 s, and the first spectrum shown in Fig. 4(b) was obtained after 35 s. It largely resembles the spectrum observed after addition of 10% D₂O to the II,III complex (Fig. 4(a)) showing the loss of bound acetate and the release of both free acetate and acetic acid. Keeping the applied potential the acetic acid peak continues to rise while the absorptions of bound (1592 cm⁻¹) and free acetate (~1570 cm⁻¹) decrease. In the final spectrum all free acetate has been converted into acetic acid and most of the bound acetate is lost. The overall process, *i.e.* immediate and delayed changes, turned out to be reversible. Re-reduction at -0.28 V quantitatively regenerated the spectrum of the intact II,II complex.

Since no spectral changes in time were observed when D₂O was added to the II,III state *after* electrolysis the delayed spectral changes can be attributed to the electrolysis of ligand-exchange products initially formed from the II,III state. Further oxidation could account for both the release of protons from existing aquo or hydroxo ligands as well as further loss of bound acetate. The sluggishness of these processes might arise from slow secondary ligand-exchange reactions as well as slow electrolysis if the electrode potential is not sufficiently positive to drive oxidation of products with diffusion controlled rate.

Effect of water on the III,III state. Fig. 5(a) compares the spectrum of [Mn₂(bpmp)(μ-OAc)₂]³⁺ in dry acetonitrile to spectra obtained in solutions with 0.1, 0.5, 2, 5, 20 and 50% D₂O added *after* oxidation at 0.82 V.

In the III,III state already small quantities of less than 1% D₂O result in the loss of about half of the bound acetate (see also Fig. 3(b)) that is not found as free acetate but exclusively as acetic acid. Further increase of the water content (1 to 50%) does not reduce the absorption of the residual acetate ligands, however. Assuming that the spectra can be essentially assigned to a specific product rather than a mixture this would indicate that the III,III state exchanges one acetate bridge much more easily but binds the remaining acetate ligand more strongly than the lower oxidation states.

Concomitantly with the loss of acetate ligands, a shift of the 1609 cm⁻¹ band of the bpmp ligand to 1606 cm⁻¹ is observed, which is not found for the lower oxidation states. The frequency is closer to but distinctively different from the value of the free ligand indicating that bpmp is still ligated to the Mn ions. The absence of free acetate indicates an at least stoichiometric release of protons. This means, that the acetate ligands in the III,III state are replaced by hydroxo or oxo ligands to compensate for the higher charge of the metal centers.

With the low D₂O content required for structural changes to occur in the III,III state the spectra could be analyzed also in the ν_(O-D) range (2500–2700 cm⁻¹, not shown) that becomes obscured with the higher D₂O content required in the lower oxidation states. No absorption attributable to the ν_(O-D) mode of OD⁻ ligands³⁵ could be observed providing evidence for the formation of O²⁻ rather than OD⁻ ligands.

Fig. 5(b) shows spectra that were obtained during electrolysis at 0.82 V of a solution containing 1% D₂O added *prior* to electrolysis. The solution of the II,II complex had been electrolyzed before at 0.32 V to prepare the II,III state. At this water content, reaction of the II,II and II,III states can be neglected, allowing for the clean preparation of the intact II,III state at 0.32 V (see Figs. 3 and 4(a)). On the other hand the reactivity of the III,III state towards water is sufficiently high to ensure almost complete release of one acetate per complex already with 1% of D₂O (see Fig. 5(a)). The first spectrum was taken after 20 s when the primary electrolysis is essentially completed and the spectrum is similar to the one obtained after subsequent addition of water to the III,III state (see above). With the potential of 0.82 V (Fig. 5(b)) applied to the cell further transformation of bound acetate into acetic acid is observed. This indicates that at this potential the products of the initial ligand-exchange reactions undergo further oxidation that eventually triggers the release of the residual acetate ligands. All acetate is found as acetic acid but it can not be decided whether additional protons are released in the course of this oxidation since already the initial ligand-exchange reaction presumably produces two equivalents of protons. The position of the 1606 cm⁻¹ band of the bpmp⁻ ligand is maintained indicating that the Mn ions are still coordinated. The changes shown in Fig. 5(b) are not reversible, however. This indicates that the oxidation products are not stable under the conditions of the strongly oxidizing potential and/or the long time scale of the experiment.

In summary, IR spectroscopy can monitor the loss of acetate ligands and the deprotonation of the water derived ligands in higher oxidation states. However, the IR spectra report average effects of samples that consist most likely of product mixtures. This required a complementary technique that could identify individual product complexes.

EC-ESI-MS

To identify products of the ligand-exchange reactions an on-line combination of electrochemistry and electrospray ionization mass spectrometry (ESI-MS) was used. The sample solutions were passed through a thin-layer electrochemical (EC) flow cell (total dead volume of 1.0–1.2 μl) in 6–12 s and transferred to the mass spectrometer *via* a silica transfer line (dead volume of 0.5 μl) in 3–6 s using a modification of a recently described EC-ESI-MS setup.²² Starting from potentials where no oxidation of [Mn₂^{II,III}(bpmp)(μ-OAc)₂]⁺ occurs the potential applied to the EC flow cell was raised in increments of 0.10 V to a final potential where no further change of the mass spectra was observed. Fig. 6 shows exemplary mass spectra in the *m/z*-range 320–390, for open circuit condition, and for different potentials applied to the working electrode (see ESI† for full range spectra). The figure compares spectra obtained in both dry acetonitrile (Fig. 6(a)–(d)) and acetonitrile–water mixture (90/10 (v/v)) (Fig. 6(e)–(h)). Based on their *m/z* value and the charge of the ion the peaks were assigned according to Table 2. The first group of peaks in the top part of the table comprises the different oxidation states of the intact [Mn₂(bpmp)(μ-OAc)₂]ⁿ⁺ while the second group of peaks lists the ligand-exchanged complexes with the suggested structure shown in Scheme 1. For all structures a preference of the water-derived ligands for bridging coordination has been assumed. Alternative structures with terminal ligands can not be excluded from the MS data but seem less likely with the open coordination sites.

In the open circuit spectrum (Fig. 6(a)) in anhydrous acetonitrile the dominating peaks at *m/z* 757.6 (see full range spectra in ESI†) and *m/z* 349.3 arise from [Mn₂^{II,III}(bpmp)(μ-OAc)₂]⁺ (**1a**) and [Mn₂^{II,III}(bpmp)(μ-OAc)₂]²⁺ (**2**). The minor peak observed at *m/z* 378.8 can be assigned to [Mn₂^{II,III}(bpmp)(μ-OAc)₂]²⁺ (**1b**). In solution complex **2** has probably aquo ligands³⁶ bound to the open coordination sites that are lost in the mass spectrometer. The fact that ligand-exchanged products were found also in

Table 2 Assignments of mass spectrometry peaks

<i>m/z</i>	Compound	Ox. state	Structure
757.5	[Mn ₂ (bpmp)(μ-OAc) ₂] ⁺	II,II	1a
378.8	[Mn ₂ (bpmp)(μ-OAc) ₂] ²⁺	II,III	1b
856.5	[Mn ₂ (bpmp)(μ-OAc) ₂] ²⁺ ·[ClO ₄] ⁻	II,III	1b
953.5	[Mn ₂ (bpmp)(μ-OAc) ₂] ³⁺ ·2[ClO ₄] ⁻	III,III	1c
349.3	[Mn ₂ (bpmp)(μ-OAc)] ²⁺	II,II	2
357.8	[Mn ₂ (bpmp)(μ-OAc)(μ-OH)] ²⁺	II,III	3
337.3	[Mn ₂ (bpmp)(μ-OH ₂ (μ-OH)] ²⁺	II,II	4
327.8	[Mn ₂ (bpmp)(μ-O)] ²⁺	II,III	5
335.8	[Mn ₂ (bpmp)(μ-O ₂)] ²⁺	III,IV	6
241.9	[N(C ₄ H ₉) ₄] ⁺ ^a	—	—
186.0	[Fe(Cp) ₂] ⁺ ^b	III	—

^a From tetrabutylammonium perchlorate supporting electrolyte. ^b From ferrocene standard.

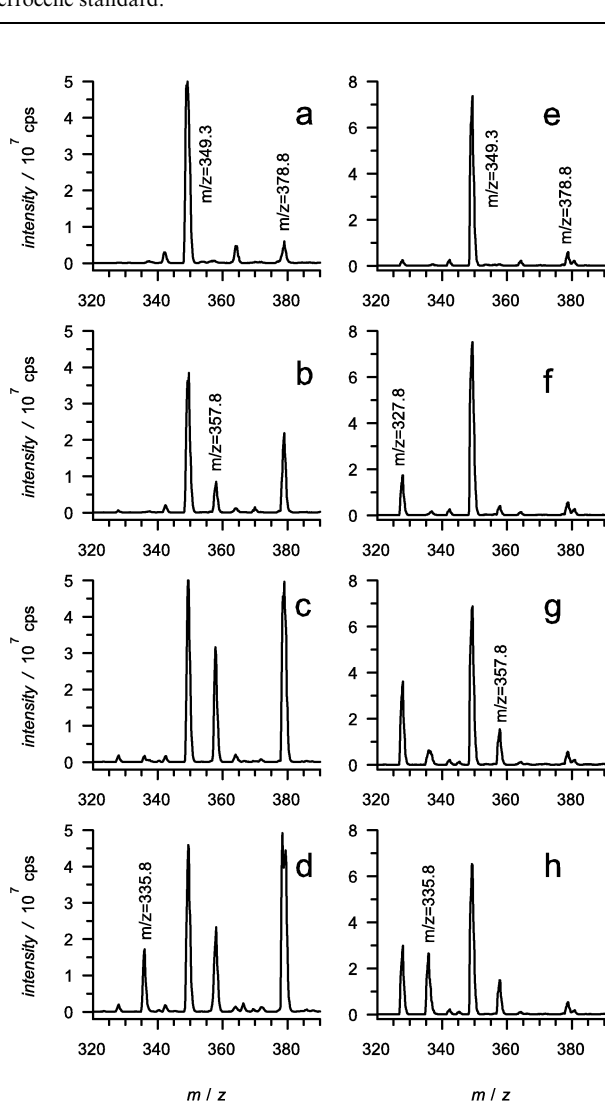
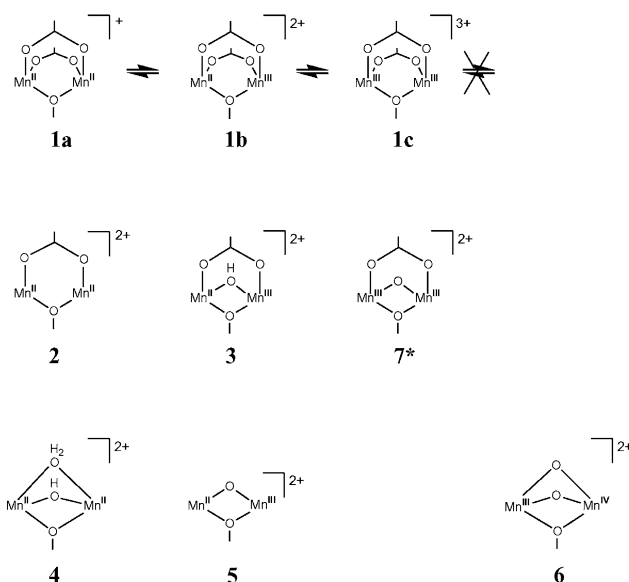


Fig. 6 EC-ESI-MS spectra of doubly charged products from [Mn₂^{III,II}(bpmp)(μ-OAc)₂]⁺ (45 μM) in CH₃CN without applied potential (a) and with 0.2 V (b), 0.7 V (c) and 1.2 V (d) applied to the EC cell. Mass spectra of doubly charged products from [Mn₂^{III,II}(bpmp)(μ-OAc)₂]⁺ (97 μM) in CH₃CN with 10% (v/v) H₂O without applied potential (e) and with 0.2 V (f), 0.4 V (g) and 0.6 V (h) applied to the EC cell.

neat acetonitrile is possibly due to exposure to atmospheric humidity in the electrospray process or small quantities of water in the acetonitrile solution. The small signal from the oxidized complex **1b** that is found in the open circuit spectra could be due to oxidation in the electrospray process or due to oxidation by oxygen. IR spectroelectrochemistry did not indicate major redox impurities in the preparation of **1a** as a reducing potential did not result in any spectral change.



* Not observed in EC-ESI-MS. Structure suggested by FT-IR.

Scheme 1

At oxidizing potentials a group of peaks was arising in the range of *m/z* 300–400 as shown in Fig. 6(b)–(d) and (f)–(h). These peaks can be ascribed to dimeric Mn complexes with the bpmp ligand and different bridging ligands (Table 2). In Scheme 1 the suggested structures are arranged according to increasing oxidation states (from left to right) and increasing degree of acetate loss (top to bottom). Beside the doubly charged complexes, minor peaks of singly charged clusters of Mn complexes and perchlorate counter ions were found at *m/z* > 800. Thus, essentially all peaks arising upon oxidation in both acetonitrile and acetonitrile–water mixtures can be ascribed to the Mn complexes given in Table 2.

Fig. 7 summarizes the results of the EC-ESI-MS measurements. The plots show the intensity of the MS peaks of the Mn complexes as a function of potential applied to the EC cell. To guide the eye the data points were fitted by simple functions that follow the trend of the data. The potential axis was calibrated with ferrocene as an external standard by defining the inflection point for the intensity of the ferrocenium peak as 0.00 V vs. Fc^{+/0}. The bar in the middle indicates the potential ranges for the oxidation states of the unaltered [Mn₂(bpmp)(μ-OAc)₂]ⁿ⁺ complex, *i.e.* **1a**, **1b** and **1c** as determined by voltammetry in anhydrous acetonitrile.

The *m/z* 757.5 peak of the starting complex **1a** is saturated at all potentials. Instead, the isotope peak with *m/z* 759.4 was plotted in Fig. 7. In this way it was ensured that all signals shown in Fig. 7 are within the dynamic range ((9–12) × 10⁷ counts s⁻¹ for 30 scans) and only the most intense signals exceed the linear range ((3–4) × 10⁷ counts s⁻¹ for 30 scans) of the mass spectrometer. As the mass spectrometer could not be calibrated for the product complexes strictly quantitative comparisons between signals from different complexes are not possible. The conversion efficiency of the flow cell that can be estimated from the depletion of **1a** at oxidizing potentials (Fig. 7(b)) is comparable to the value of 50% that has been found earlier for the same setup.²²

Oxidation in acetonitrile. The signal of the oxidation product **1b** (*m/z* 378.8) rises at potentials above *E*_{1/2}(1) and reaches a plateau at *ca.* 0.8 V. No depletion of the signal from **1b** was observed even at potentials above *E*_{1/2}(2) possibly due to the incomplete electrolysis resulting in comproportionation of **1c** and **1a** to give **1b**. This could also explain that only a very weak signal from **1c** (*m/z* 953, not shown) is observed at potentials above 0.9 V.

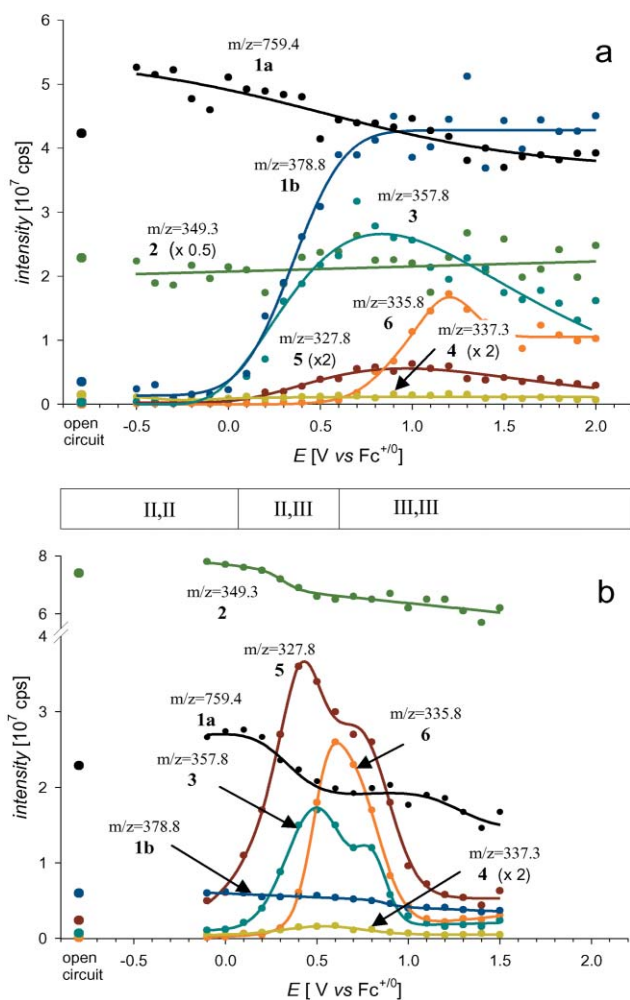


Fig. 7 Intensities of EC-ESI-MS peaks assigned to manganese complexes **1–6** as a function of potential applied to the EC cell in CH_3CN (a) and CH_3CN with 10% (v/v) H_2O (b).

The II,II complexes **2** and **4** are the only ligand-exchange products that can be found in solutions with no applied potential (see open circuit signal) indicating that they are formed directly from **1a**. That they are not depleted over the whole potential range might indicate that they are formed from **1a** after the EC cell.

The formation of the II,III complexes **3** and **5** is triggered by the first oxidation step as their signals are rising concomitantly with **1b**. As the potential for the second oxidation (**1b** \rightarrow **1c**) is passed a III,IV complex, **6**, is formed. This indicates that **1c** is a precursor of **6** but no sizable signal from the intact III,III complex is observed and no ligand-exchanged III,III complex is found. It is conceivable that the intact III,III complex (**1c**) is sufficiently oxidizing to oxidize not only unelectrolyzed II,II complex but possibly also ligand-exchanged III,III complexes thereby generating the III,IV complex **6**. Thus, **1c** would be consumed by a homogeneous reaction before it reaches the mass spectrometer.

The occurrence of ligand-exchange products in the open circuit spectrum in neat acetonitrile can be explained by either exposure to atmospheric humidity in the electrospray process or by small quantities of water in the acetonitrile solution. The first possibility implies that ligand-exchange reactions occur only after the sample passed the electrochemical cell, while the latter includes the option of secondary electrolysis steps after ligand exchange.

Oxidation in acetonitrile–water. In solutions with no applied potential the II,II complex **2** is the dominating ligand-exchange product. The structure of **2** with aquo ligands most likely

occupying the open coordination sites in solution is in agreement with the IR results in the II,II state (Fig. 3(a)) that demonstrate the loss of acetate ligands without deprotonation of water-derived ligands

The signal of the first oxidation product **1b** does not rise above the open circuit level when the potential of the first oxidation is passed. Instead, the predominant II,III product signals arise from **3** and **5** that might be formed by reaction of **1b** with water, consistent with the results in neat acetonitrile. Complexes **3** and **5** could be also formed to some extent from **2** which shows some depletion above 0.1 V. The structures of **3** and **5** with deprotonated water-derived ligands are in agreement with the IR spectra (Fig. 4(a)) that show a mixture of free acetate and acetic acid when **1b** is exposed to water.

The III,IV complex **6** is formed clearly below the potential of the second oxidation of the mother compound indicating that **6** is not formed from **1c** in the acetonitrile–water (90/10) mixture. Depletion of **3** and **5** around the peak of **6** suggests that their further oxidation leads to the formation of **6**. In response to oxidation to their III,III states, **3** and **5** most probably deprotonate (in solution also **5** has water ligands) and a product such as **7** might be formed, as suggested by the IR data. The deprotonation could allow for further oxidation at the same or only slightly higher potential that eventually results in the III,IV complex **6**. This would explain the absence of ligand-exchanged III,III complexes in the mass spectra even if these would undergo no or less complete comproportionation with the starting material due to the lower oxidation potentials compared to the unaltered complex **1c**.

From Scheme 1 it can be seen that in a given oxidation state ligand exchange does not necessarily result in a lower overall charge compared to the intact complex (compare **3** with **1b** or **1a** with **2** and **4**). The ligand-exchange reactions, however, facilitate further oxidation that is coupled to deprotonation of the water-derived ligands. Thus the III,IV-complex **6** has only one more positive charge than the starting II,II-complex **1a**. Similarly the III,III-complex **7** in which the oxo bridge is deprotonated has a lower charge than the diacetato complex **1c**.

With respect to the formation of the most oxidized complex, **6**, the EC-ESI-MS measurements suggest that already at a water content of 10% the dominating pathway is the oxidation of products such as **3** and **5**, which were formed by ligand exchange in the II,III state **1b**. Only at lower water content **6** should be formed predominantly *via* the intact III,III complex (**1c**).

Conclusions

By the combination of electrochemistry with IR spectroscopy and ESI-MS we were able to monitor the loss of acetate ligands from $[Mn_2(bpmp)(\mu-OAc)_2]^+$ in different oxidation states and identify products of the ligand-exchange reactions. Our results show that the II,II and II,III states are less prone to acetate loss in solutions of low water content while the III,III state releases acetate ligands already with much less water. This finding is in agreement with our earlier conclusion based on voltammetric data that the ligand-exchange reactions with a water content $\leq 10\%$ are most efficiently triggered by the second oxidation step to the III,III state. In a given oxidation state the ligand-exchange reactions do not lower the overall charge compared to the intact complex but, as expected, the water-derived ligands that replace the acetate bridges are increasingly deprotonated in the higher oxidation states thereby facilitating further oxidation.

The di- μ -oxo bridged III,IV dimer, $[Mn_2(bpmp)(\mu-O)_2]^{2+}$ generated by electro-oxidation of $[Mn_2(bpmp)(\mu-OAc)_2]^+$ can be assigned to the strongly spin coupled III,IV dimer detected in the EPR studies^{18,19} in the course of photo-oxidation of $[Mn_2(bpmp)(\mu-OAc)_2]^+$. The mechanism of the formation of the III,IV dimer seems to depend on the water content of the solution. $[Mn_2(bpmp)(\mu-O)_2]^{2+}$ can be formed *via* ligand-exchange reactions starting from the intact III,III

complex $[\text{Mn}_2(\text{bpmp})(\mu\text{-OAc})_2]^{3+}$ if little water is present but also *via* ligand-exchange products of the lower oxidation states if high water content favors ligand exchange in these states. In the latter case the potential required for the formation of the di- μ -oxo bridged III,IV dimer drops even below the potential of the III,III/II,III couple (0.61 V vs. $\text{Fc}^{+/0}$) of the di- μ -acetato complex. The formation of the III,IV dimer by photo-oxidation with $[\text{Ru}(\text{bpy})_3]^{2+}$ (0.90 V vs. $\text{Fc}^{+/0}$) could be accomplished by either pathway but under the conditions of the EPR experiments (10–90% water) ligand exchange in the II,II and II,III state of $[\text{Mn}_2(\text{bpmp})(\mu\text{-OAc})_2]^{n+}$ is most likely the dominating mechanism.

Acknowledgements

Stenbjörn Styring, Ann Magnuson, Ping Huang (Uppsala), Joakim Höglblom (Lund), Magnus Anderlund, Björn Åkermark and Licheng Sun (Stockholm) are gratefully acknowledged for discussions and continuous collaboration, and M. A. and L. S. for providing samples of $[\text{Mn}_2(\text{bpmp})(\mu\text{-OAc})_2][\text{ClO}_4]$ and $[\text{Mn}_2(\text{bpmp})(\mu\text{-OAc})_2][\text{ClO}_4]_2$.

Financial support from the following organisations is gratefully acknowledged: the Swedish Energy Agency, the Swedish Research Council and the Swedish Foundation for Strategic Research. L. H. gratefully acknowledges a research fellow position from The Royal Swedish Academy of Sciences.

References

- V. L. Pecoraro and W.-Y. Hsieh, *Met. Ions Biol. Syst.*, 2000, **37**, 429–504.
- S. Mukhopadhyay, S. K. Mandal, S. Bhaduri and W. H. Armstrong, *Chem. Rev.*, 2004, **104**, 3981–4026.
- J. Limburg, V. A. Szalai and G. W. Brudvig, *J. Chem. Soc., Dalton Trans.*, 1999, 1353–1362.
- K. Wieghardt, *Angew. Chem.*, 1989, **101**, 1179–1198.
- W. Ruettinger and G. C. Dismukes, *Chem. Rev.*, 1997, **97**, 1–24.
- L. Sun, L. Hammarström, B. Åkermark and S. Styring, *Chem. Soc. Rev.*, 2001, **30**, 36–49.
- L. Sun, H. Berglund, R. Davydov, T. Norrby, L. Hammarström, P. Korall, A. Börje, C. Philouze, K. Berg, A. Tran, M. Andersson, G. Stenhagen, J. Mårtensson, M. Almgren, S. Styring and B. Åkermark, *J. Am. Chem. Soc.*, 1997, **119**, 6996–7004.
- M. L. A. Abrahamsson, H. B. Baudin, A. Tran, C. Philouze, K. E. Berg, M. K. Raymond-Johansson, L. Sun, B. Åkermark, S. Styring and L. Hammarström, *Inorg. Chem.*, 2002, **41**, 1534–1544.
- K. E. Berg, A. Tran, M. K. Raymond, M. Abrahamsson, J. Wolny, S. Redon, M. Andersson, L. Sun, S. Styring, L. Hammarström, H. Toftlund and B. Åkermark, *Eur. J. Inorg. Chem.*, 2001, 1019–1029.
- L. Sun, M. K. Raymond, A. Magnuson, D. LeGourrierec, M. Tamm, M. Abrahamsson, P. H. Kenez, J. Mårtensson, G. Stenhagen, L. Hammarström, S. Styring and B. Åkermark, *J. Inorg. Biochem.*, 2000, **78**, 15–22.
- D. Burdinski, E. Bothe and K. Wieghardt, *Inorg. Chem.*, 2000, **39**, 105–116.
- M. P. Klein, K. Sauer and V. K. Yachandra, *Photosynth. Res.*, 1993, **38**, 265–277.
- R. D. Britt, in *Oxygenic Photosynthesis: The Light Reactions*, ed. D. R. Ort and C. F. Yocum, Kluwer Academic, Dordrecht, 1996, vol. 4, pp. 137–164.
- M. J. Baldwin and V. L. Pecoraro, *J. Am. Chem. Soc.*, 1996, **118**, 11325–11326.
- H. H. Thorp, J. E. Sarneski, G. W. Brudvig and R. H. Crabtree, *J. Am. Chem. Soc.*, 1989, **111**, 9249–9250.
- T. Tanase and S. J. Lippard, *Inorg. Chem.*, 1995, **34**, 4682–4690.
- L. Dubois, R. Caspar, L. Jacquamet, P.-E. Petit, M.-F. Charlot, C. Baffert, M.-N. Collomb, A. Deronzier and J.-M. Latour, *Inorg. Chem.*, 2003, **42**, 4817–4827.
- P. Huang, A. Magnuson, R. Lomoth, M. Abrahamsson, M. Tamm, L. Sun, B. van Rotterdam, J. Park, L. Hammarström, B. Åkermark and S. Styring, *J. Inorg. Biochem.*, 2002, **91**, 159–172.
- P. Huang, J. Höglblom, M. F. Anderlund, L. Sun, A. Magnuson and S. Styring, *J. Inorg. Biochem.*, 2004, **98**, 733–745.
- V. Kertesz and G. J. Van Berkel, *Electroanalysis*, 2001, **13**, 1425–1430.
- F. Zhou and G. J. Van Berkel, *Anal. Chem.*, 1995, **67**, 3643–3649.
- C. F. Bökman, C. Zettersten, P. J. R. Sjöberg and L. Nyholm, *Anal. Chem.*, 2004, **76**, 2017–2024.
- H. Diril, H. R. Chang, M. J. Nilges, X. Zhang, J. A. Potenza, H. J. Schugar, S. S. Isied and D. N. Hendrickson, *J. Am. Chem. Soc.*, 1989, **111**, 5102–5114.
- L. Tang and P. Kebarle, *Anal. Chem.*, 1993, **65**, 3654–3668.
- P. Kebarle and L. Tang, *Anal. Chem.*, 1993, **65**, 972A–986A.
- A. M. Bond, R. Colton, A. D'Agostino, A. J. Downard and J. C. Traeger, *Anal. Chem.*, 1995, **67**, 1691–1695.
- X. Xu, W. Lu and R. B. Cole, *Anal. Chem.*, 1996, **68**, 4244–4253.
- M. Suzuki, M. Mikuriya, S. Murata, A. Uehara, H. Oshio, S. Kida and K. Saito, *Bull. Chem. Soc. Jpn.*, 1987, **60**, 4305–4312.
- G. B. Deacon and R. J. Phillips, *Coord. Chem. Rev.*, 1980, **33**, 227–250.
- K. Wieghardt, U. Bossek, B. Nuber, J. Weiss, J. Bonvoisin, M. Corbella, S. E. Vitols and J. J. Girerd, *J. Am. Chem. Soc.*, 1988, **110**, 7398–7411.
- K. Wieghardt, U. Bossek, J. Bonvoisin, P. Beauvillain, J. J. Girerd, B. Nuber, J. Weiss and J. Heinze, *Angew. Chem.*, 1986, **98**, 1026–1027.
- K. Wieghardt, U. Bossek, D. Ventur and J. Weiss, *J. Chem. Soc., Chem. Commun.*, 1985, 347–349.
- J. C. Smith, E. Gonzalez-Vergara and J. B. Vincent, *Inorg. Chim. Acta*, 1997, **255**, 99–103.
- S. Blanchard, G. Blondin, E. Riviere, M. Nierlich and J.-J. Girerd, *Inorg. Chem.*, 2003, **42**, 4568–4578.
- Z. Shirin, V. G. Young, Jr. and A. S. Borovik, *Chem. Commun.*, 1997, 1967–1968.
- A. Boisen, A. Hazell and C. J. McKenzie, *Chem. Commun.*, 2001, 2136–2137.